JOURNAL OF Materials CHEMISTRY

# Hydrothermal synthesis, structural, spectroscopic and magnetic studies of a lamellar phosphate: $Ba(MnPO_4)_2 \cdot H_2O$

**Jaione Escobal,[a] José L. Mesa,[a] José L. Pizarro,[b] Luis Lezama,[a] Roger Olazcuaga[c] and Teófilo Rojo*[a]**

[a]*Departamentos de Química Inorgánica y* [b]*Mineralogía-Petrología, Facultad de Ciencias, Universidad del País Vasco, Apdo. 644, E-48080, Bilbao, Spain. E-mail: qiproapt@lg.ehu.es*
[c]*Institut de Chimie de la Matière Condenseé de Bordeaux, 33608 Pessac, France*

***Received 12th April 1999, Accepted 30th June 1999***

$Ba(MnPO_4)_2 \cdot H_2O$ has been prepared by hydrothermal synthesis and characterized by spectroscopic and magnetic techniques. Its crystal structure has been solved from X-ray powder diffraction data by using direct methods and refined with the Rietveld method. The compound crystallizes in the monoclinic system in the $C2$ space group with unit cell parameters, $a=9.457(1)$, $b=4.984(1)$, $c=8.346(1)$ Å and $\beta=92.07(1)^\circ$. The structure consists of a two-dimensional network of $MnO_6$ octahedra, linked by phosphate anions and water molecules, which form chains along the |010| direction. The luminescence properties of Mn(II) in the compound are studied and the values of $Dq$ and Racah parameters $B$ and $C$ have been calculated. The EPR spectra recorded on a polycrystalline sample at different temperatures show isotropic signals with $g$-values of 2.0. The intensity of the EPR signals increases with decreasing temperature down to 45 K and at lower temperatures rapidly decreases. Magnetic measurements show the presence of antiferromagnetic interactions. An analysis of the magnetic behaviour was carried out considering a theoretical model for antiferromagnetic chains with spin $S=5/2$. Similar values for the $J$-exchange parameter inside the chains ($J/k=-2.0$ K) and for the $J'$-exchange parameter between neighbouring chains ($zJ'/k=-2.0$ K) are observed. These results suggest that the compound can be considered as a non-regular two-dimensional magnetic system.

## Introduction

Phosphates with the structural unit $(MPO_4)^-$, where M is a divalent transition metal, can give rise to a large variety of framework structures.[1] Moreover, the presence of transition metals in the structure opens up the possible application of these materials as shape-selective redox catalysts.[2] In this way, several open-framework materials with cobalt(II) ions partially incorporated into the structure have been used as catalysts in the autoxidation of cylohexane[2] and *p*-cresol.[3]

Open-framework phosphates and arsenates with different monovalent ions ($Li^+$, $Na^+$, $K^+$, $NH_4^+$,...) incorporated between the sheets or into channels have been reported over recent years.[4–12] Some of them exhibit interesting magnetic properties, which can be understood as three-dimensional (3D)[11,13] or intermediate 2D–3D magnetic systems.[8] A canting phenomenon has been observed in the layered $NH_4Mn(XO_4)\cdot H_2O$ (X = P, As) dittmarites.[14,15] The magnetic structure of the $LiMn(XO_4)(OD)$ (X = P, As; D = deuterium) phases, in which the $Li^+$ ions lie within the small channels of the three-dimensional framework, has been determined.[16] The latter compounds exhibit global antiferromagnetic behaviour, with ferromagnetic intrachain interactions between the Mn(III) ions. A variety of mixed-metal phosphates and arsenates with divalent transition metal and alkaline-earth metal ions have been also prepared and studied.[17] The magnetic properties of the $Ba(NiXO_4)_2$ (X = P, As) compounds have been extensively studied showing the presence of two-dimensional antiferromagnetic interactions.[18] However, hydrated phosphates with general formula $M'(MPO_4)_2\cdot nH_2O$, where M′ = alkaline-earth ion and M = divalent transition metal are less known. Unfortunately, even if good crystals for X-ray structure determination were obtained in several cases,[19,20] pure phases have not been prepared. This fact has precluded any study of the physical properties of these materials.

As a part of our investigation concerning the synthesis and magnetic and spectroscopic studies of layered phosphates and arsenates with transition metal ions, we have prepared $Ba(MnPO_4)_2\cdot H_2O$ under hydrothermal conditions. In this work, we report on the structural characterization of $Ba(MnPO_4)_2\cdot H_2O$, together with spectroscopic and magnetic studies. As far as we are aware, this compound is the first layered hydrated barium manganese phosphate.

## Experimental

### Synthesis and characterization

$Ba(MnPO_4)_2\cdot H_2O$ was synthesized under hydrothermal conditions. An aqueous solution of $MnCl_2\cdot 4H_2O$ (4.38 mmol), $H_3PO_4$ (8.40 mmol) and $Ba(OH)_2\cdot H_2O$ (2.19 mmol) was prepared. The pH of the solution was increased by adding methylamine up to pH ≈ 11. The mixture was heated at 170 °C for 72 h in a poly(tetrafluoroethylene)-lined stainless steel container under autogeneous pressure, filled to *ca.* 75% volume capacity. A fine polycrystalline light-pink solid was separated by filtration, washed with water and acetone and dried over $P_2O_5$ for 12 h.

Manganese, barium and phosphorus contents were determined by inductively coupled plasma atomic emission spectroscopy (ICP-AES) analysis. The results were consistent with the stoichiometry $Ba(MnPO_4)_2\cdot H_2O$ (Found: Ba, 30.0; Mn, 24.0; P, 13.4. Calc.: Ba, 30.2; Mn, 24.1; P, 13.6%). Thermogravimetry of $Ba(MnPO_4)_2\cdot H_2O$ shows only one mass loss step in the temperature range 200–500 °C of 4%. This loss can be attributed to the water molecule present in the compound (calc., 3.95%). There was no further mass loss between 500 and 800 °C. Attempts to identify the nature of the inorganic residue in the Powder Diffraction File[21] have been unsuccessful.

### X-Ray crystallography

The X-ray powder diffraction pattern of $Ba(MnPO_4)_2 \cdot H_2O$, used for the Rietveld analysis, was collected with a Siemens diffractometer with Bragg–Brentano geometry. A small portion of the compound was spread on a flat-plate to attenuate the effect of the preferred orientation in the spectrum. Cu-K$\alpha$ radiation was employed with steps of 0.02° in 2$\theta$ and fixed-time counting of 12 s. Preliminary attempts to refine the crystal structure of $Ba(MnPO_4)_2 \cdot H_2O$ by using the atomic coordinates of the isostructural $Ba(CoPO_4)_2 \cdot H_2O$ as a starting model were unsuccessful. Although the *R*-factors obtained were consistent, we observed unrealistic Mn–O and P–O bond distances for the compound. This fact is probably due to the different ionic radii of the cations. Consequently, we solved the structure using an *ab initio* method. The FULLPROF program (pattern matching mode)[22] was used to obtain the integrated intensities of the reflections observed in the X-ray powder diffraction spectrum. These intensities were employed in the structural resolution using the SIRPOW92 program[23] (direct methods). The atomic coordinates obtained for all non-hydrogen atoms present in $Ba(MnPO_4)_2 \cdot H_2O$ were refined using the Rietveld method (FULLPROF program). The final atomic coordinates are similar to those reported for the isostructural $Ba(CoPO_4)_2 \cdot H_2O$.[19] Details of the process are given in Table 1. The observed, calculated and difference X-ray powder diffraction patterns are shown in Fig. 1.

### Physicochemical characterization techniques

Thermogravimetric measurements were performed in a Perkin-Elmer system 7 DSC-TGA instrument. Crucibles containing *ca.* 20 mg of sample were heated at 5 °C $min^{-1}$ under dry nitrogen atmosphere in the temperature range 30–800 °C. The IR spectrum (KBr pellet) was obtained with a Nicolet FT-IR 740 spectrophotometer in the range 400–4000 $cm^{-1}$. Luminescence measurements were carried out in a Spectrofluorometer Fluorolog-2 SPEX 1680, model F212I at 8 K. The excitation source was a high pressure xenon lamp emitting between 200 and 1200 nm. The diffuse reflectance spectrum was measured at room temperature on a Cary 2415 spectrometer in the range 210–2000 nm. A Bruker ESP 300 spectrometer was used to record the EPR spectra from room temperature to 4.2 K. The temperature was stabilised by an Oxford Instrument (ITC 4) regulator. The magnetic field was measured with a Bruker BNM 200 gaussmeter and the frequency inside the cavity was determined using a Hewlett-Packard 5352B microwave frequency counter. Magnetic measurements of powdered samples were performed in the temperature range 1.8–300 K, using a Quantum Design MPMS-7 SQUID magnetometer. The magnetic field was *ca.* 0.1 T, a value lying within the range of linear dependence of the magnetization *vs.* magnetic field even at 1.8 K.

**Table 1** Summary of crystallographic data and least-squares refinement for $Ba(MnPO_4)_2 \cdot H_2O$

| | |
|---|---|
| Compound | $Ba(MnPO_4)_2 \cdot H_2O$ |
| *M* | 455.2 |
| Crystal system | Monoclinic |
| Space group | *C*2 (no. 5) |
| *a*/Å | 9.457(1) |
| *b*/Å | 4.984(1) |
| *c*/Å | 8.346(1) |
| $\beta$/° | 92.07(1) |
| *V*/Å$^3$ | 393.1(1) |
| *T*/K | 298 |
| $\lambda$(Cu-K$\alpha$) | 1.5418 |
| *Z* | 2 |
| $D_c$/g $cm^{-3}$ | 2.31 |
| 2$\theta$ range/° | 5–110 |
| 2$\theta$ Step-scan increment/° | 0.02 |
| Time per step/s | 12 |
| No. of reflections | 566 |
| No. of structural parameters | 24 |
| No. of profile parameters | 12 |
| $R_p = \Sigma\lvert yi_{obs} - (1/c) yi_{calc}\rvert / \Sigma yi_{obs}$ | 16.8 |
| $R_{wp} = [\Sigma wi\lvert yi_{obs} - (1/c) yi_{calc}\rvert^2 / \Sigma wi[yi_{obs}]^2]^{1/2}$ | 20.2 |
| $R_B = \Sigma\lvert I_{obs} - I_{calc}\rvert / \Sigma I_{obs}$ | 7.0 |
| GOF | 1.34 |

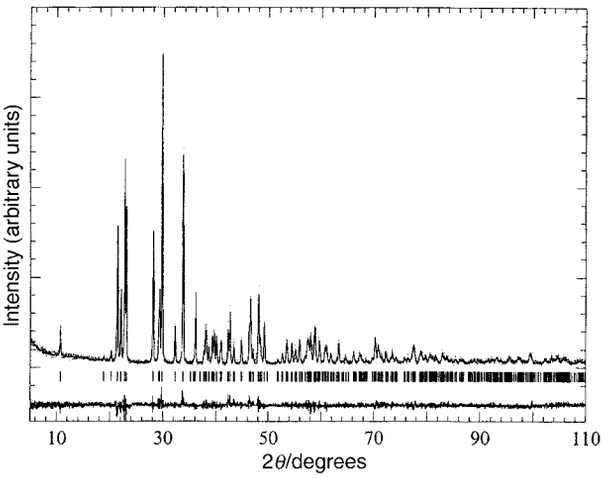


**Fig. 1** Observed, calculated and difference X-ray powder diffraction patterns of $Ba(MnPO_4)_2 \cdot H_2O$. The observed data are shown by the dots, the calculated pattern is shown by the solid line and the difference spectrum is presented in the lower region.

## Results and discussion

### Structural study

Atomic coordinates for the $Ba(MnPO_4)_2 \cdot H_2O$ compound are given in Table 2 and interatomic bond distances and angles are presented in Table 3.

The structure of $Ba(MnPO_4)_2 \cdot H_2O$ is built from $MnO_6$ octahedra edge-sharing with $PO_4$ tetrahedra, to form infinite two-dimensional sheets stacked along the |001| direction [Fig. 2(a)]. The $Ba^{2+}$ ions are located in the interlayer region and act as counterions of the $(MnPO_4 \cdot H_2O)^-$ sheets. Within the inorganic layer [Fig. 2(b)] the $MnO_6$ polyhedra form chains, along the |010| direction, which are interconnected by water molecules and phosphate anions. An important structural feature of this compound is the simultaneous presence of –Mn–O–P–O–Mn– and –Mn–O–Mn– bridges. The latter linkage through water molecules is not common in phosphate compounds. $NH_4Mn(XO_4) \cdot H_2O$ (X = P, As) layered phases also have water molecules in their structures, but they do not have Mn–O–Mn bridges. The water molecules act as pendant groups on the octahedral Mn(II) centres.[7,15]

$Ba(MnPO_4)_2 \cdot H_2O$ contains distorted $MnO_6$ octahedra with Mn–O distances ranging from 2.04(2) to 2.55(1) Å, and *cis*-O–

**Table 2** Fractional atomic coordinates and equivalent isotropic displacement parameters for $Ba(MnPO_4)_2 \cdot H_2O$

| Atom | Site | *x* | *y* | *z* | $B_{eq}$[a]/Å$^2$ |
|---|---|---|---|---|---|
| Ba | 2b | 0.5 | 0.62800 | 0.0 | 1.80(8) |
| Mn | 4c | 0.3364(5) | 0.067(1) | 0.3422(5) | 1.2(1) |
| P | 4c | 0.3446(7) | 0.127(2) | 0.7419(8) | 0.8(2) |
| O(1) | 2a | 0.5 | −0.250(4) | 0.5 | 1.3(2) |
| O(2) | 4c | 0.330(1) | 0.251(3) | 0.564(2) | 1.3(2) |
| O(3) | 4c | 0.492(1) | 0.168(3) | 0.804(1) | 1.3(2) |
| O(4) | 4c | 0.748(1) | 0.791(3) | 0.849(2) | 1.3(2) |
| O(5) | 4c | 0.682(2) | 0.821(3) | 0.255(2) | 1.3(2) |

[a] $B_{eq} = (8\pi^2/3)\,[U_{22} + 1/(\sin^2\beta)(U_{11} + U_{33} + 2U_{13}\cos\beta)]$.

**Table 3** Selected bond distances (Å) and angles (°) for $Ba(MnPO_4)_2 \cdot H_2O$[a]

| | | | |
|---|---|---|---|
| $MnO_6$ octahedron | | $BaO_{10}$ decahedron | |
| Mn–O(1) | 2.55(1) | $Ba–O(3)^{v}/O(3)^{viii}$ | 3.15(2) ×2 |
| $Mn–O(2)/O(2)^{i}$ | 2.07(2)/2.38(1) | $Ba–O(3)^{vi}/O(3)^{ii}$ | 2.82(2) ×2 |
| $Mn–O(3)^{ii}$ | 2.13(1) | $Ba–O(4)^{vi}/O(4)^{ii}$ | 2.82(2) ×2 |
| $Mn–O(4)^{iii}$ | 2.23(1) | $Ba–O(4)^{vii}/O(4)^{ix}$ | 3.14(1) ×2 |
| $Mn–O(5)^{iv}$ | 2.04(2) | $Ba–O(5)/O(5)^{x}$ | 2.86(2) ×2 |
| $PO_4$ tetrahedron | | | |
| P–O(2) 1.61(2) | | | |
| P–O(3) 1.48(1) | | | |
| $P–O(4)^{iv}$ 1.54(2) | | | |
| $P–O(5)^{iii}$ 1.54 (2) | | | |
| | | | |
| $MnO_6$ octahedron | | $PO_4$ tetrahedron | |
| $O(1)–Mn–O(2)^{i}$ | 79.4(4) | $O(2)–P–O(4)^{iv}$ | 107.4(9) |
| $O(1)–Mn–O(3)^{ii}$ | 88.8(4) | $O(2)–P–O(5)^{iii}$ | 112.8(9) |
| $O(1)–Mn–O(4)^{iii}$ | 100.5(5) | O(2)–P–O(3) | 108.3(8) |
| O(1)–Mn–O(2) | 81.3(5) | $O(5)^{iii}–P–O(3)$ | 106(1) |
| $O(5)^{iv}–Mn–O(3)^{ii}$ | 101.6(6) | $O(5)^{iii}–P–O(4)^{iv}$ | 114.6(9) |
| $O(5)^{iv}–Mn–O(2)$ | 90.2(6) | $O(3)–P–O(4)^{iv}$ | 107.0(9) |
| $O(5)^{iv}–Mn–O(4)^{iii}$ | 83.9(6) | | |
| $O(5)^{iv}–Mn–O(2)^{i}$ | 93.1(6) | | |
| $O(2)–Mn–O(2)^{i}$ | 87.6(5) | | |
| $O(2)–Mn–O(3)^{ii}$ | 117.1(6) | | |
| $O(2)^{i}–Mn–O(4)^{iii}$ | 66.6(5) | | |
| $O(4)^{iii}–Mn–O(3)^{ii}$ | 89.8(6) | | |
| $O(1)–Mn–O(5)^{iv}$ | 168.8(5) | | |
| $O(2)–Mn–O(4)^{iii}$ | 153.1(6) | | |
| $O(2)^{i}–Mn–O(3)^{ii}$ | 150.8(6) | | |

[a]Symmetry codes: i = $-x+1/2$, $y+1/2$, $-z+1$; ii = $-x+1$, $y$, $-z+1$; iii = $-x+1$, $y-1$, $-z+1$; iv = $x-1/2$, $y-1/2$, $z$; v = $x$, $y+1$, $z-1$; vi = $x$, $y$, $z-1$; vii = $x-1/2$, $y-1/2$, $z-1/2$; viii = $-x+1$, $y+1$, $-z+1$; ix = $-x+3/2$, $y-1/2$, $-z+1$; x = $-x+1$, $y$, $-z$.

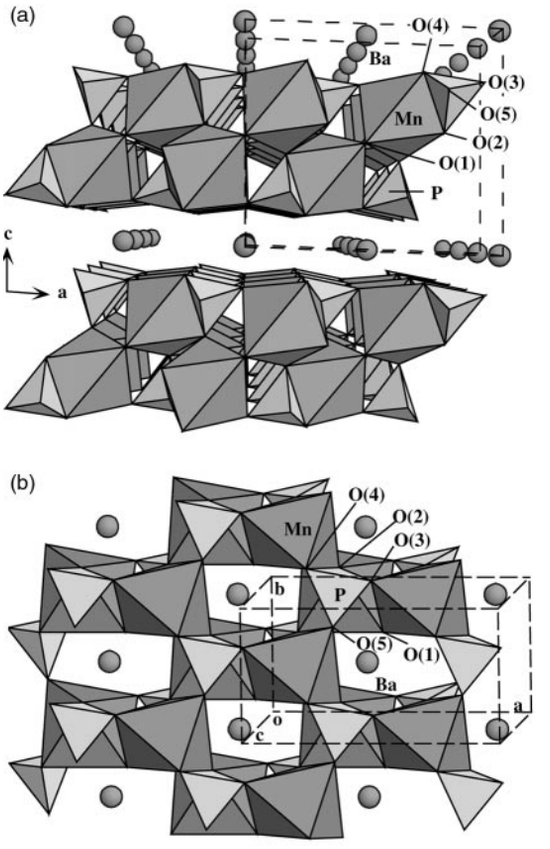


**Fig. 2** (a) Crystal structure of $Ba(MnPO_4)_2 \cdot H_2O$ showing the layered structure. (b) Schematic view of a layer showing the chains of Mn(II) ions.

Mn–O angles ranging from 66.5(5) to 117.1(6)°. In the isostructural $Ba(CoPO_4)_2 \cdot H_2O$ the Co–O distances and the *cis*-O–Co–O angles range from 2.027(4) to 2.397(5) Å and from 67.3(2) to 116.2(2)°, respectively.[19] The four equatorial bonds $Mn–O(2)/O(2)^{i}/O(3)^{ii}/O(4)^{iii}$ are 2.07(2), 2.38(1), 2.13(1) and 2.23(1) Å, respectively, and correspond to oxygen atoms from $PO_4$ tetrahedra [Fig. 2(b)]. The axial $O(5)^{iv}$ oxygen is provided by a $PO_4$ tetrahedron [$Mn–O(5)^{iv}$ 2.04(2) Å] but the remaining axial vertex is formed by the O(1) from the coordinated water molecule [Mn–O(1) 2.55(1) Å]. The distortion of this $MnO_6$ coordination polyhedron from an octahedron ($\Delta = 0$) to a trigonal prism ($\Delta = 1$), calculated by quantification of the Muetterties and Guggenberger description,[24,25] is $\Delta = 0.23$, which indicates a topology near to octahedral. The $PO_4$ groups can be described as distorted tetrahedra. The P–O distances and the O–P–O angles have a mean value of 1.54(5) Å and 109(3)°, respectively. The $Ba^{2+}$ ions are located between the inorganic layers and establish up to ten bonds with oxygen atoms, with distances ranging from 2.82(2) to 3.15(2) Å. A similar result has been obtained for $Ba(CoPO_4)_2 \cdot H_2O$,[19] where the Ba–O bond distances range from 2.763(4) to 3.237(4) Å.

Oxidation states of Mn, Ba and P were calculated as a sum of bond valences, $s$, using the equations: $s = (r/r_0)^{-N}$ and $s = \exp[(r_0 - r)/B]$, where $r_0$, $N$ and $B$ are empirical parameters [$r_0$(Mn–O) = 1.798, $N = 5.6$; $r_0$(Ba–O) = 2.297, $N = 7.0$ and $r_0$(P–O) = 1.62, $B = 0.36$] and $r$ is the refined bond length.[26] The calculated oxidation states are 1.98, 1.83 and 5.00 for Mn, Ba and P, respectively, which are in good agreement with those expected for the elements present in $Ba(MnPO_4)_2 \cdot H_2O$.

## IR, luminescence and UV–VIS spectroscopy

The IR spectrum of $Ba(MnPO_4)_2 \cdot H_2O$ shows bands corresponding to the vibrations of the water molecule and the phosphate anions. The strong band centred at 3435 $cm^{-1}$ corresponds to the stretching mode of water. The bending mode of water is observed at *ca.* 1595 $cm^{-1}$. Moreover, the spectrum shows three important groups of bands. The bands observed in the region 1100–675 $cm^{-1}$ are attributed to the stretching vibration modes of the $PO_4^{3-}$ groups. The asymmetric $\nu_{as}$(P–O) stretching modes appear at 1060, 1015 and 950 $cm^{-1}$ while the symmetric $\nu_s$(P–O) stretch is detected at 685 $cm^{-1}$. The asymmetric deformation vibrations [$\delta_{as}$(O–P–O)] are observed at 620, 585 and 550 $cm^{-1}$. The splitting of these bands is due to the distortion of the $PO_4$ tetrahedra as observed from the structural data. These results were also observed in other related phosphates, in which the $PO_4^{3-}$ anions are in a low local symmetry.[8,27]

Luminescence measurements of the $Mn^{2+}$ ion in $Ba(MnPO_4)_2 \cdot H_2O$ have been carried out at 8 K. Fig. 3(a) shows the emission spectrum of the compound obtained at $\lambda_{ex} = 411$ nm. It exhibits a unique red emission peaking at 660 nm which is characteristic of an octahedral environment for $Mn^{2+}$ ($d^5$) ions. The excitation spectrum ($\lambda_{em} = 660$ nm) [Fig. 3(b)] reveals a spectral distribution of bands corresponding to the excited levels of $Mn^{2+}$ [$^4T_1(^4G)$: 512 nm; $^4T_2(^4G)$: 438 nm; $^4A_1$,$^4E(^4G)$: 411 nm; $^4T_2(^4D)$: 376 nm; $^4E(^4D)$: 348 nm]. These values are in accord with those generally observed for $Mn^{2+}$ in an octahedral site.[28,29] The diffuse reflectance spectrum of $Ba(MnPO_4)_2 \cdot H_2O$ exhibits several very weak spin-forbidden d–d bands, at *ca.* 345, 375, 410 and 435 nm, as expected for a high spin $d^5$ cation,[30] in good agreement with the luminescence results.

Taking into account the results of the luminescence spectroscopy, the $Dq$ and Racah parameters have been calculated by fitting the experimental frequencies to an energy level diagram for an octahedral $d^5$ high spin system.[30] The values obtained are $Dq = 850$, $B = 535$ and $C = 3930$ $cm^{-1}$. These values are in the range usually found for octahedrally coordinated Mn(II) compounds.[31]

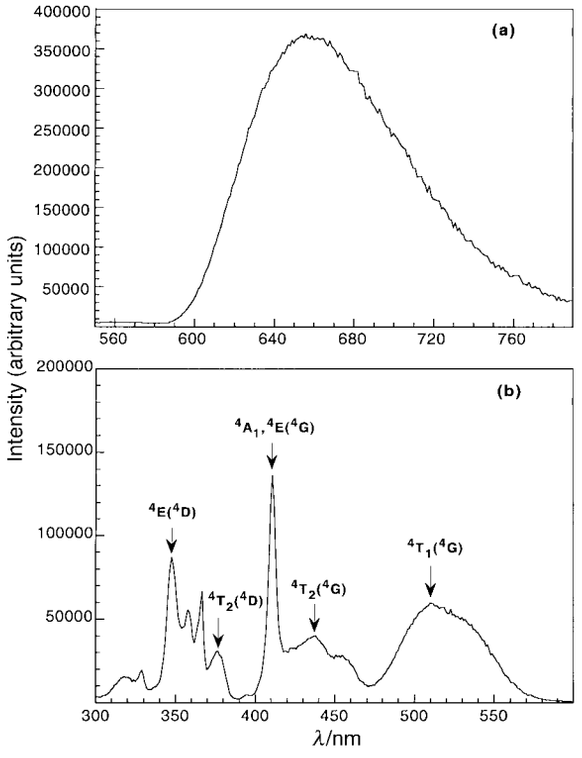


**Fig. 3** (a) Emission spectrum ($\lambda_{exc}=411$ nm) and (b) excitation spectrum ($\lambda_{em}=660$ nm) of $Ba(MnPO_4)_2{\cdot}H_2O$ at 8 K.

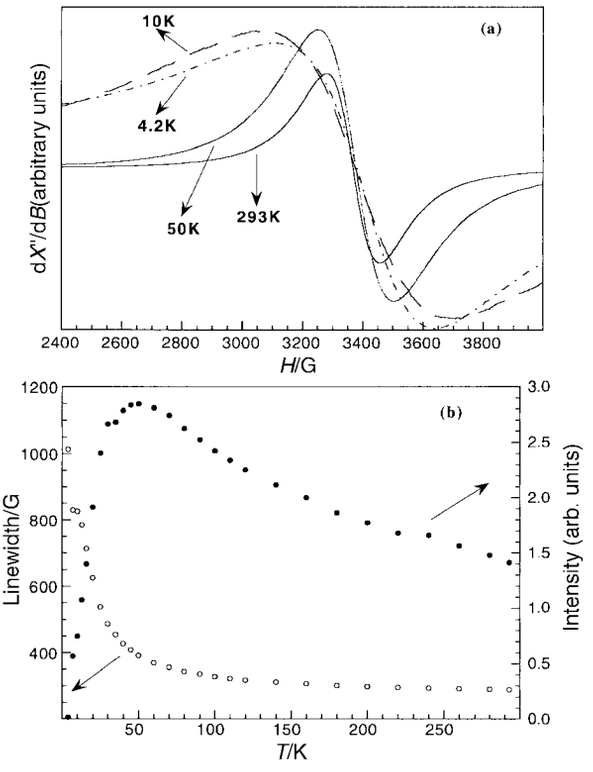


**Fig. 4** (a) Powder X-band EPR spectra of $Ba(MnPO_4)_2{\cdot}H_2O$, at different temperatures. (b) Temperature dependence of the intensity of the signal and the linewidth curves for $Ba(MnPO_4)_2{\cdot}H_2O$ compound.

## EPR and magnetic properties

EPR spectra of $Ba(MnPO_4)_2{\cdot}H_2O$ have been recorded on a powdered sample at X-band between 4.2 and 300 K and are shown in Fig. 4(a). The spectra remain essentially unchanged upon cooling the sample from 300 to 50 K. Below this temperature, however, the signal broadens and loses intensity. The spectra are isotropic with a *g*-value of *ca.* 2.0, which remains unchanged with temperature. This *g*-value is characteristic of octahedrally coordinated Mn(II). The temperature dependence of the intensity and the linewidth of the signals calculated by fitting the experimental spectra to Lorentzian curves are displayed in Fig. 4(b). The intensity of the signal increases with decreasing temperature and reaches a maximum at *ca.* 45 K then rapidly decreases. This fact suggests the existence of antiferromagnetic coupling in the compound. The linewidth increases slightly from room temperature to *ca.* 50 K probably owing to dipolar homogeneous broadening. When the temperature is further decreased the linewidth increases significantly. These results are in good agreement with those observed for other antiferromagnets, in which the linewidth also increases drastically when the Neel temperature is reached.[32–36]

Variable-temperature magnetic susceptibility measurements were performed on a powdered sample in the range 1.8–300 K. Plots of $\chi_m$ and $\chi_m T$ *vs.* $T$ for $Ba(MnPO_4)_2{\cdot}H_2O$ are shown in Fig. 5. The thermal evolution of $\chi_m$ follows the Curie–Weiss law at temperatures $>50$ K, with $C_m=4.25$ cm$^3$ K mol$^{-1}$ and $\theta=-21.5$ K, exhibiting a maximum in $\chi_m$ at 16.5 K. This result together with the continuous decrease in the $\chi_m T$ values are indicative of antiferromagnetic exchange couplings in the compound.

Considering the structural features of this compound in which the interlayer distances between the $(MnPO_4{\cdot}H_2O)^-$ sheets are $>5$ Å, together with the broad maximum observed in the magnetic susceptibility curve at *ca.* 16 K, a three-dimensional (3D) magnetic model can be disregarded from analysis of the magnetic behaviour. However, a two-dimensional magnetic model such as the 2D-regular planar

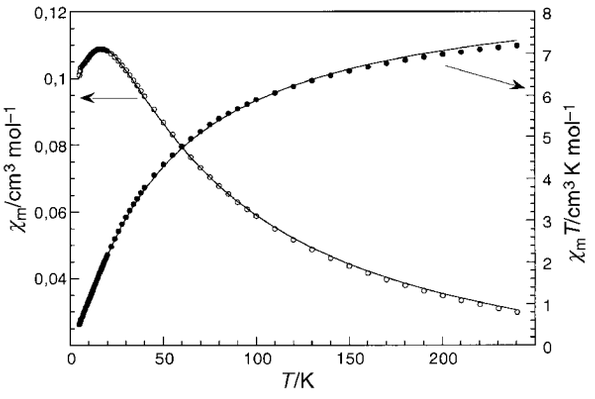


**Fig. 5** Temperature dependence of $\chi_m$ and $\chi_m T$ for $Ba(MnPO_4)_2{\cdot}H_2O$. The circles are the experimental values and the full lines represent the theoretical values for a Heisenberg chain of $S=5/2$.

honeycomb arrangement as shown in Fig. 6 could be considered for an $S=5/2$ antiferromagnetic system. This model supposes the existence of only one magnetic exchange pathway between the manganese(II) ions arranged within the layers. The results obtained in the fit are not ideal probably due to the presence of two different magnetic exchange pathways (see Fig. 6) with two different *J*-exchange parameters. From this point of view and taking into account the existence of interconnected chains of Mn(II) ions in the sheets, a Heisenberg model for infinite chains with $S=5/2$ was used in the magnetic analysis of this compound. Eqn. (1) given by Fisher and Dingle[37,38]

$$\chi = [Ng^2\beta^2 S(S+1)/3kT][(1-n)/(1+n)] \qquad (1)$$

can be proposed as a theoretical approach to the magnetic behaviour of $Ba(MnPO_4)_2{\cdot}H_2O$, where $n=(T/T_0)-\coth(T_0/T)$ and $T_0=[2JS(S+1)]/k$, where $k$ is the Boltzmann constant, $N$ is Avogadro's number and $\beta$ is the Bohr magneton. However, the

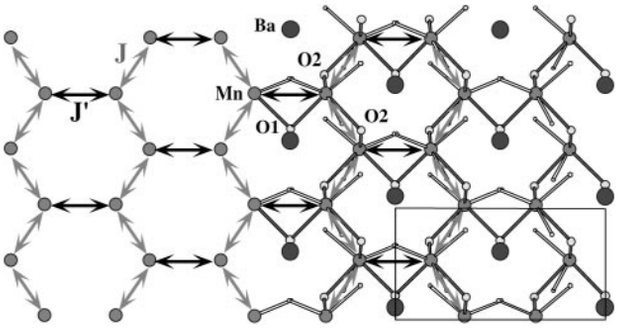


**Fig. 6** Schematic representation of the Mn(II) chains showing the 2D-honeycomb arrangement of the cations and the *J*-exchange parameters considered in the fit of the magnetic data.

fit of the experimental data to this theoretical model still does not give a good fit. Finally, upon considering the existence of magnetic interactions between neighbouring chains, and introducing a *J'*-exchange parameter, good agreement between the experimental data and the theoretical model was obtained (Fig. 5). The best fit parameters have been found to be $J/k = -2.0$ K and $zJ'/k = -2.0$ K, with $g = 2.0$ from the EPR data. The high value obtained for the *J'*-exchange parameter is noteworthy, with $z = 2$ from the structural results, in comparison to the value of the *J* parameter. This fact indicates that the theoretical model must be considered with caution. However, although the obtained *J* and *J'* exchange parameters can be considered as an approximate result, the good fit obtained for the magnetic data allow us to conclude that the compound can be regarded as a non-regular two-dimensional magnetic system with magnetic interactions propagated in the *ab*-plane, with magnetic exchange along the chains (*b*-axis) being stronger than that in an approximately perpendicular direction.

## Conclusion

The crystal structure of $Ba(MnPO_4)_2 \cdot H_2O$ has been solved from X-ray diffraction data by using direct methods and then refined by the Rietveld procedure. The compound exhibits a layered structure with $Ba^{2+}$ ions placed in the interlayer region. The sheets are formed by $MnO_6$ octahedra linked to $PO_4$ tetrahedra giving rise to infinite chains of Mn(II) along the *b*-axis. The chains of Mn(II) ions are interconnected simultaneously by $PO_4^{3-}$ anions and water molecules, this latter linkage being unusual in phosphate compounds. Using $Mn^{2+}$ as a local probe, the luminescent properties at 8 K are consistent with a unique octahedral site for this cation. X-Band EPR powder spectra have been recordered at different temperatures and show isotropic signals characteristic of octahedrally coordinated Mn(II) ions. Study of the intensity of EPR signals with temperature suggests antiferromagnetic interactions in this compound. Magnetic measurements from room temperature to 1.8 K confirm the EPR results. The magnetic behaviour of $Ba(MnPO_4)_2 \cdot H_2O$, analyzed by using different magnetic models, is consistent with a two-dimensional non-regular system, in which two different magnetic exchange pathways must be considered.

## Acknowledgements

This work was financially supported by the Ministerio de Educación y Ciencia and Universidad del País Vasco/EHU (grants PB97-0640 and 169.310-EB149/98, respectively), which we gratefully acknowledge. We thank P. Amorós (Univ. Valencia, Spain) for the X-ray powder diffraction measurements and F. Guillen (I.C.M.C.B., Pessac, France) for luminescence measurements at low temperature. J. E. thanks the UPV/EHU for a doctoral fellowship.

## References

1 T. E. Gier and G. D. Stucky, *Nature*, 1991, **349**, 508.
2 S. S. Lin and H. S. Weng, *Appl. Catal. A*, 1993, **105**, 289.
3 J. Dakka and R. A. Sheldon, *Netherlands Pat.* 9 200 968, 1992.
4 P. Y. Feng, X. H. Bu and G. D. Stucky, *J. Solid. State Chem.*, 1997, **129**, 328.
5 P. Y. Feng, X. H. Bu and G. D. Stucky, *J. Solid State Chem.*, 1997, **131**, 160.
6 P. Y. Feng, X. H. Bu, S. H. Tolbert and G. D. Stucky, *J. Am. Chem. Soc.*, 1997, **119**, 2497.
7 S. G. Carling, P. Day and D. Visser, *Inorg. Chem.*, 1995, **34**, 3917.
8 A. Goñi, J. L. Pizarro, L. M. Lezama, G. E. Barberis, M. I. Arriortua and T. Rojo, *J. Mater. Chem.*, 1996, **6**, 421.
9 A. Pujana, J. L. Pizarro, L. Lezama, A. Goñi, M. I. Arriortua and T. Rojo, *J. Mater. Chem.*, 1998, **8**, 1055.
10 I. Abrahams and K. S. Easson, *Acta Crystallogr., Sect. C*, 1993, **49**, 925.
11 J. L. Mesa, J. L. Pizarro, L. Lezama, J. Escobal, M. I. Arriortua and T. Rojo, *J. Solid State Chem.*, 1998, **141**, 508.
12 A. M. Buckley, S. T. Bramwell and P. Day, *Z. Naturforsch., Teil B*, 1998, **44**, 1053.
13 A. Goñi, L. Lezama, G. E. Barberis, J. L. Pizarro, M. I. Arriortua and T. Rojo, *J. Magn. Magn. Mater.*, 1996, **164**, 251.
14 S. G. Carling, P. Day and D. Visser, *Solid State Commun.*, 1993, **88**, 135.
15 J. L. Mesa, J. L. Pizarro, L. Lezama, A. Goñi, M. I. Arriortua and T. Rojo, *Mater. Res. Bull.*, in press.
16 M. A. G. Aranda, S. Bruque, J. P. Attfield, F. Palacios and R. B. Von Dreele, *J. Solid State Chem.*, 1997, **132**, 202.
17 A. Moqine, A. Boukhari and J. Darriet, *J. Solid State Chem.*, 1993, **107**, 362, and references therein.
18 L. P. Regnault, J. Y. Henry, J. Rossat-Mignod and D. De Combariel, *J. Magn. Magn. Mater.*, 1980, **15–18**, 1021.
19 X. Bu, P. Feng and G. D. Stucky, *J. Solid State Chem.*, 1997, **131**, 387.
20 H. Effenberger, *J. Solid State Chem.*, 1999, **142**, 6.
21 Powder Diffraction File, Compiled by International Centre for Diffraction Data, Swarthmore, PA, 1995.
22 J. Rodriguez-Carvajal, FULLPROF, Program Rietveld Pattern Matching Analysis of Powder Patterns, ILL Grenoble, 1994, unpublished work.
23 A. Antomare, G. Cascarano, C. Giacovazzo, A. Guagliardi, M. C. Burla, G. Polidori and M. Camalli, *J. Appl. Crystallogr.*, 1994, **27**, 738.
24 E. L. Muetterties and L. J. Guggenberger, *J. Am. Chem. Soc.*, 1974, **96**, 1748.
25 R. Cortés, M. I. Arriortua, T. Rojo, X. Solans and D. Beltrán, *Polyhedron*, 1986, **5**, 1987.
26 I. D. Brown, *Structure and Bonding in Crystals*, ed. M. O'Keeffe and A. Navrotsky, Academic Press, New York, 1981, vol. 2, p. 1.
27 A. Goñi, J. Rius, M. Insausti, L. Lezama, J. L. Pizarro, M. I. Arriortua and T. Rojo, *Chem. Mater.*, 1996, **8**, 1052.
28 L. E. Orgel, *J. Chem. Phys.*, 1955, **23**, 1004.
29 Y. Tanabe and S. Sugano, *J. Phys. Soc. Jpn.*, 1954, **9**, 753.
30 A. B. P. Lever, *Inorganic Electronic Spectroscopy*, Elsevier Science Publishers B.V., Amsterdam, Netherlands, 1984.
31 K. E. Lawson, *J. Chem. Phys.*, 1966, **44**, 4159.
32 H. W. Wijn, L. R. Walker, J. L. Daris and H. Guggenheim, *J. Solid State Commun.*, 1972, **11**, 803.
33 P. M. Richards and M. B. Salamon, *Phys. Rev. B: Condens. Matter*, 1974, **9**, 32.
34 A. Escuer, R. Vicente, M. A. S. Goher and F. Mautner, *Inorg. Chem.*, 1995, **34**, 5707.
35 A. Bencini and D. Gatteschi, *EPR of Exchange Coupled Systems*, Springer-Verlag, Berlin–Heidelberg, 1990.
36 T. T. P. Cheung, Z. G. Soos, R. E. Dietz and F. R. Merrit, *Phys. Rev. B: Condens. Matter*, 1978, **17**, 1266.
37 M. E. Fisher, *Am. J. Phys.*, 1964, **32**, 343.
38 R. Dingle, M. E. Lines and S. L. Holt, *Phys. Rev.*, 1969, **187**, 643.

*Paper 9/02871D*